Preparation of flake-like polyaniline/montmorillonite nanocomposites and their application for removal of Cr(VI) ions in aqueous solution

Jun Chen · Xiaoqin Hong · Yongteng Zhao · Youyi Xia · Diankai Li · Qianfeng Zhang

Abstract In this study, flake-like polyaniline/montmorillonite (PANI/MMT) nanocomposites with rough surface were successfully prepared by in situ chemical oxidation polymerization during which poly(2-acrylamido-2-methylpropanesulfonic acid), a polymer acid, on the surface of clay platelets was used as dopant of PANI and played a 'bridge' role to combine PANI with clay. Flake thickness and surface roughness of PANI/MMT composites decreased with the increase of montmorillonite/aniline feeding ratio. The effects of operating parameters including pH, contact time, Cr(VI) concentration, and adsorbent dose were studied. The pseudo-second-order equation and three adsorption isotherms including Langmuir, Freundlich, and Temkin equations were applied to determine the adsorption rate and capacity. The results show that the flake-like PANI/MMT nanocomposites exhibited a high adsorption capacity (167.5 mg/g). The excellent adsorption characteristic of flake-like PANI/MMT nanocomposites will render it a highly efficient and economically viable adsorbent for Cr(VI) removal.

J. Chen (✉) · Q. Zhang
School of Chemistry and Chemical Engineering, Institute of Molecular Engineering & Applied Chemistry, Anhui University of Technology, Ma'anshan 243002, China
e-mail: junchen@ahut.edu.cn

X. Hong · Y. Zhao · Y. Xia
School of Chemistry and Chemical Engineering, Anhui University of Technology, Ma'anshan 243002, China

D. Li
School of Materials Science and Engineering, Anhui University of Technology, Ma'anshan 243002, China

Introduction

Heavy metals are potentially hazardous to human health even in minute quantities. Chromium is a typical heavy metal pollutant in industrial wastewater. In aqueous solution Cr is found in two stable oxidation states such as trivalent Cr(III) and hexavalent Cr(VI). The hexavalent form is toxic, carcinogenic, and mutagenic in nature, whereas Cr(III) is less toxic. Cr(VI) is used extensively in industries such as electroplating, tanning, and textile and thus is widely present in the effluents of these industries [1].

There are various methods used for the removal of Cr(VI) from aqueous solutions, such as chemical precipitation, membrane filtration, ion exchange, and adsorption [2–7]. Among these methods, adsorption has been widely studied because it is easy to operate and cost-effective [8]. Many adsorbents have been studied for removal of Cr(VI) from aqueous solutions, including activated carbons [9, 10], zeolites [11], clay minerals [12, 13], organic resin [14], chitosan [15, 16], and waste products from industrial operations such as fly ash [17] and coal [18]. Most of these adsorbents, however, are hard to satisfy the demands of high efficiency, low cost, and no second contamination at the same time.

Polyaniline, a well-known conducting polymer, has been attracting more attention in multidisciplinary fields including electrochromic devices, rechargeable batteries, sensors, electromagnetic shielding devices, and anticorrosion coatings because of their nontoxicity, good environmental stability, low cost, and ease of preparation [19]. Polyaniline has shown its good prospect for removing heavy metal ions because it carries large amounts of amine and imine functional groups which can chelate metal ions and also can adsorb anionic metal species through electrostatic or hydrogen bonding [20]. Polyaniline doped with sulfuric acid was used to remove Cr(VI) from aqueous solution.

Adsorption equilibrium is attained within a short contact time of 1.5 h and the maximum uptake of Cr(VI) was 95.79 mg/g [21]. Chowdhury et al. [22] used synthetic HCl-doped polyaniline (particle size approximate to 0.20 mm) for the removal and recovery of Cr(VI) from contaminated wastewater. The mono-layer adsorption capacity was 22.2 mg of Cr(VI) per gram of doped polyaniline at 4.75 pH and 25 °C. One-dimensional polyaniline nanowire/tubes with rough surface were also prepared for removal of Cr(VI) in aqueous solution. This kind of PANI nanostructure can not only remove Cr(VI) rapidly and effectively but also be easily regenerated for reuse [23]. However, bare PANI particles are easily aggregated in aqueous solutions, which results in low adsorption capacity and slow kinetics. In order to avoid aggregation of PANI properly and enhance the adsorption capacity, PANI composites were subject to extensive studies by in situ polymerization of aniline in the presence of other materials. Polyaniline/humic acid composites were prepared by adding humic acid into the chemical polymerization process of aniline. The humic acid played an important role in modifying the morphology, preventing the aggregation of PANI, and improving the uptake properties of Cr(VI) on the composite in pH 3.0–7.0 [24]. Chowdhury et al. [25] prepared polyaniline/silica gel composite absorbent with high surface area by 'grafting to' method. The capacity can be up to 135 mg/g even at very low level of Cr(VI) (70 mg/L). Core–shell polyaniline/polystyrene nanocomposite was synthesized and used for removal of Cr(VI) from aqueous solutions. The optimum conditions for Cr(VI) removal are achieved with pH 4, adsorbent dosage of 15 g/L, and 30 min equilibrium time [26]. Polyaniline/natural fiber composite adsorbents were also developed for Cr(VI) removal [27, 28].

Montmorillonite is a natural, abundant, and inexpensive mineral which has unique layered structure, large specific surface area, chemical and mechanical stability as well as high cation exchange capacity (CEC). The characteristics have made the MMT excellent adsorbent material for a few heavy metals [12, 13, 29]. For practical application, it is desirable to develop low-cost adsorbent with high capacity for Cr(VI). In this respect, micro/nanostructured adsorbents with enhanced adsorption capacity have been of increasing interest [30, 31]. In this report, PANI/MMT nanocomposites with flake-shaped morphology have been developed by in situ chemical oxidation polymerization with MMT platelets as the scaffold. The as-obtained flake-like PANI/MMT nanocomposites can be used as adsorbents for removal of Cr(VI) from an aqueous solution and exhibited a high adsorption capacity. This study not only provides a simple approach to controllably fabricate PANI/MMT micro/nanostructures, but also gives an excellent Cr(VI) adsorbent, which is of great importance for applications in the treatment of heavy metal wastewater.

Experimentals

Materials

Aniline (ANI), ammonium persulfate (APS), 1,5-diphenylcarbohydrazide, potassium dichromate, sodium hydroxide, sulfuric acid, and hydrochloric acid were purchased from Sinopharm Chemical Reagent Co., Ltd (China). All chemicals were of analytical grade and used without further purification. 2-Acrylamido-2-methylpropanesulfonic acid (AMPS) was kindly supplied by All-plus Chemical Co., Ltd (China). Pristine Na^+-MMT clay (PGW, cationic (Na^+) exchange capacity of 145 meq/100 g) was purchased from Nanocor Inc. (USA). The polymerizable tertiary amine (GMA-DEA, chemical structure seen in Fig. 1) used for clay surface modification was synthesized as described elsewhere [32].

Surface modification of pristine MMT

The organic modification of Na^+-MMT clay with GMA-DEA was carried out as follows: 15 g of Na^+-MMT clay was dispersed in 450 mL distilled water by stirring overnight at room temperature. An excess of GMA-DEA (6.45 g, 1.2 CEC) was dissolved in 50 mL of distilled water and then continuously added dropwise to the clay dispersion. The pH value of the mixture was adjusted to 3 using hydrochloric acid. The mixture was stirred for 6 h. Afterward, the modified MMT clay, hereinafter referred to as GMA-DEA-MMT, were filtrated and washed several times to remove excess GMA-DEA and hydrochloric acid, and then redispersed in 500 mL distilled water.

150 mL 2 wt% GMA-DEA-MMT dispersion was charged into a 250-mL round-bottom flask equipped with a mechanical stirrer, a condenser, and nitrogen inlet. 3.0 g AMPS was then added and stirred under a nitrogen atmosphere by purging for 30 min. The initiator, 0.03 g APS (dissolved in 5 mL of distilled water), was finally introduced in the reactor and the polymerization allowed to proceed at 70 °C for 4 h under a slow stream of nitrogen. The resulted dispersion was centrifuged and washed repeatedly with distilled water to remove the ungrafted poly(AMPS). The obtained modified MMT clay (hereinafter referred to as PAMPS-g-MMT) was then redispersed in 120 mL distilled water.
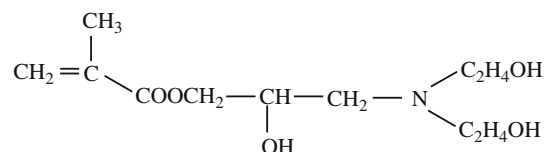

Fig. 1 Chemical structure of GMA-DEA

Preparation of flake-like PANI/MMT nanocomposites

PANI/MMT was prepared by the chemical oxidation method as follows: certain amount of the PAMPS-g-MMT was dispersed in 80 mL of 0.5 mol/L hydrochloric acid. Then, 0.8 g aniline monomer was added and stirred for 30 min. The polymerization started by introduction of APS solution (1.96 g APS in 20 mL of 0.5 mol/L hydrochloric acid) dropwise. An overnight reaction was allowed to ensure completion of polymerization. The resultant precipitate was filtered and sequentially washed with copious amounts of 0.1 mol/L hydrochloric acid and industrial alcohol until the filtrate was clear. Finally, the product was dried at 50 °C in an oven.

According to the aforementioned approach, numerous samples of the PANI/MMT nanocomposites with different MMT/aniline feeding ratio were obtained. The feeding ratio of MMT/aniline is defined using Eq. (1):

$$\text{MMT/Aniline feeding ratio} = \frac{W_{\text{MMT}}}{W_{\text{Aniline}}} \times 100 \text{ wt\%} \qquad (1)$$

Removal of Cr(VI) ions

All the adsorption experiments were carried out at room temperature. An aqueous stock solution of Cr(VI) (500 mg/L) was prepared by dissolving potassium dichromate in deionized water. Aqueous Cr(VI) solutions with different concentrations were obtained by diluting the stock solution with water. The pH values of solution were well adjusted by NaOH and H_2SO_4. The concentration of Cr(VI) was analyzed by spectrophotometer using 1,5-diphenylcarbazide as the complexing agent at the wavelength of 540 nm (GB 7467-87) [21, 33].

For the effect of pH values and PANI/MMT concentration of solution on the removal capacity experiment, 50 mg of the as-synthesized PANI/MMT nanocomposites was ultrasonically dispersed into 50 mL of Cr(VI) solution for 1 min with different pH values and concentrations, and then the mixture was stirred magnetically. After 2.5 h of contact the solution was centrifuged and supernatant liquid analyzed for residual Cr(VI). The Cr(VI) removal efficiency was determined using Eq. (2):

$$\%\text{Removal} = \left(\frac{C_0 - C_e}{C_0}\right) \times 100, \qquad (2)$$

where C_0 and C_e are the initial and equilibrium concentrations (mg/L) of Cr(VI), respectively.

For the kinetics experiment, the as-synthesized PANI/MMT (200 mg) was ultrasonically dispersed into 200 mL of Cr(VI) solution for 1 min at pH 2. Next, an appropriate amount of the solution was taken out at predetermined intervals and centrifuged quickly. The supernatant liquids were used for analyzing Cr(VI) concentration. The adsorption capacity of the PANI/MMT q_t (mg/g) at time t was obtained from Eq. (3):

$$q_t = \left(\frac{C_0 - C_t}{m}\right)V, \qquad (3)$$

where m is the PANI/MMT mass (g), V is the volume of solution (L), and C_t is the concentration of Cr(VI) at any time t (mg/L).

The adsorption isotherm study was carried out with different initial Cr(VI) concentrations ranging from 25 to 250 mg/L at pH 2 while maintaining the PANI/MMT amount of 1 g/L and contact time of 2.5 h. The amount of Cr(VI) adsorbed was calculated using Eq. (4):

$$q_e = \left(\frac{C_0 - C_e}{m}\right)V, \qquad (4)$$

where q_e is the equilibrium adsorption capacity (mg/g).

Desorption experiments were also conducted to investigate the recovery of PANI/MMT adsorbent. Initially for adsorption of Cr(VI), 0.05 g PANI/MMT was treated with 50 mL of 100 ppm Cr(VI) at pH 2. Desorption of Cr(VI) loaded PANI/MMT adsorbent was performed using 50 mL of 0.1 M NaOH solution. Thereafter, for regeneration of the sorption sites of adsorbent, PANI/MMT was contacted with 2 M HCl solution. The regenerated PANI/MMT adsorbent was examined for four consecutive adsorption–desorption cycles to verify the reusability of the adsorbent.

Characterization

Scanning electron microscopy (SEM) equipped with an energy dispersive analysis system of X-ray spectrometer (EDX) (Nova NanoSEM 430, FEI Company) was employed to study the morphology and distribution of elemental components of PANI/MMT nanocomposites. Transmission electron microscopy (TEM) measurements were performed on a JEOL JEM-2100 transmission electron microscope with an accelerating voltage of 200 kV by a GATAN digital photography system. MMT and PANI/MMT nanocomposites in a powder form were embedded in KBr (Uvasol, Merck) matrix and analyzed on a Fourier transform infrared spectroscopy (FTIR) spectrometer (Nicolet 6700). X-ray diffraction patterns of pristine MMT and modified MMT in a powder form were investigated with a Japanese Rigaku D/max 2500PC X-ray diffractometer with Cu Kα radiation at 40 kV and 40 mA. Data were collected at a scan rate of 1.0°/min with 0.02° step size in the 2θ range of 1°–10°.

Results and discussion

Modification of Na$^+$-MMT

In order to confirm that surface modification of pristine Na$^+$-MMT was successfully carried out, the pristine Na$^+$-MMT, GMA-DEA-MMT, and PAMPS-g-MMT were analyzed by FTIR and XRD. Results are shown in Figs. 2 and 3. Characteristic bands of MMT at 1040, 467, and 521 cm^{-1}, corresponding to Si–O bonds' stretching and Si–O bonds' bending, exist in all the spectra. The absorption band at 1720 cm^{-1}, corresponding to C=O stretching vibration, appears in the spectrum of the GMA-DEA-MMT clay, which indicates the existence of GMA-DEA in GMA-DEA-MMT clay. The increment of the d spacing from 1.32 nm for pristine Na$^+$-MMT to 1.51 nm for GMA-DEA-MMT indicates an intercalated system with insertion of GMA-DEA into clay layers (shown in Fig. 3). The absorption band at 1550 cm^{-1}, corresponding to C–N stretching vibration of poly(AMPS), appears in the spectrum of the PAMPS-g-MMT and the d spacing also increases from 1.51 nm for GMA-DEA-MMT to 1.67 nm for PAMPS-g-MMT, which both indicate that poly(AMPS) successfully modified the MMT by surface grafting polymerization.

Characterization of flake-like PANI/MMT

Typical SEM images of the obtained PANI/MMT are shown in Fig. 4a, b, which show highly uniform flake-like structures. The SEM images indicate that the typical lateral dimensions of the flakes are several hundred nanometers to a few microns and the thickness of the flake is about several tens of nanometers. It also can be seen from the SEM images that the surface of flake-like PANI/MMT is rough, which is consistent with the TEM image of Fig. 4c.

Figure 5 shows the morphologies of PANI/MMT synthesized with different feeding ratio of MMT/aniline. It can be seen that the PANI/MMT obtained by reducing the MMT/aniline feeding ratio to 12.5 % comprises two kinds of morphologies (shown in Fig. 5a). One is the flake-like structure, which is similar to the typical sample shown in Fig. 4. The other is the irregular grain structure, which appears to be formed by the aggregate of several PANI particles. When the MMT/aniline feeding ratio increased, the prepared PANI/MMT composites all show the flake-like structure with decreased flake thickness and lower surface roughness.

The main elemental compositions of such flake-like PANI/MMT are shown in the EDX results in Fig. 4d. The existence of C, O, Cl, Si, and Al is verified, suggesting it is a composite of PANI and MMT. The chemical structures of the PANI/MMT composites are characterized by FTIR spectra as shown in Fig. 6. The characteristic bands of PANI in composites clearly observed at 1560 and 1480 cm^{-1} were assigned to the C=C stretching of the quinoid and benzenoid rings, respectively. The adsorption bands at 1300 and 1240 cm^{-1} correspond to C–N stretching vibration of secondary amine of PANI backbone and bipolaron structure related to the C–N stretching vibration, respectively [34]. The absorption band at 1110 cm^{-1} is due to the C–H in plane bending. Additionally, characteristic bands of MMT at 1040 and 467 cm^{-1}, corresponding to Si–O bonds' stretching and Si–O bonds' bending, exist in all the spectra of composites. The IR results proved the formation of PANI/MMT nanocomposites, which is in accord with the EDX result.
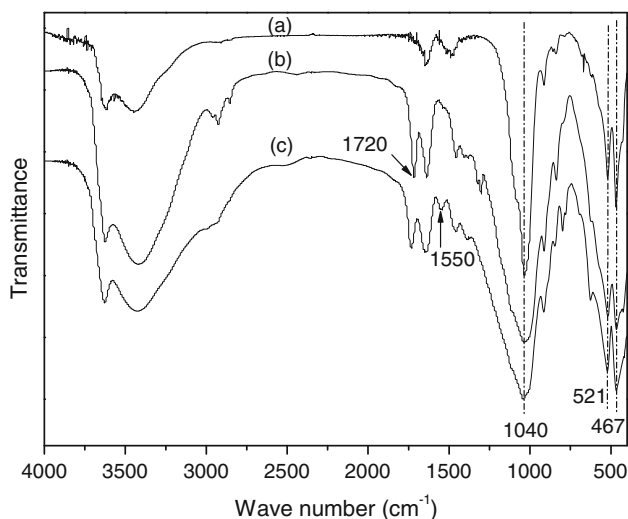

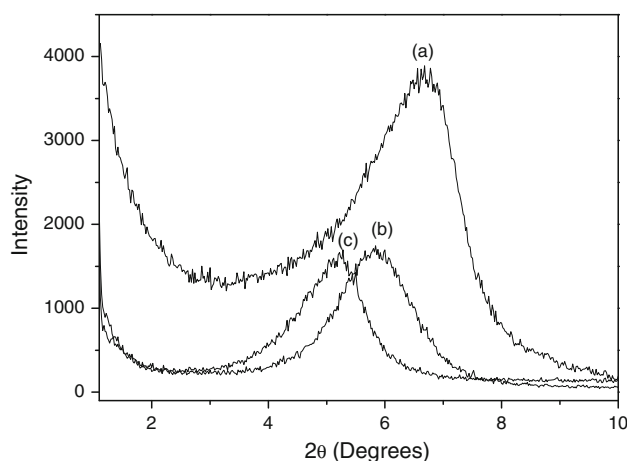**Fig. 2** FTIR spectra of Na$^+$-MMT (*a*), GMA-DEA-MMT (*b*) and PAMPS-g-MMT (*c*)

Fig. 3 X-ray diffraction curves of Na$^+$-MMT (*a*), GMA-DEA-MMT (*b*) and PAMPS-g-MMT (*c*)

Fig. 4 a Low-magnification SEM, **b** high-magnification SEM, **c** EDX and **d** TEM images of flake-like PANI/MMT with the MMT/aniline feeding ratio of 25 %
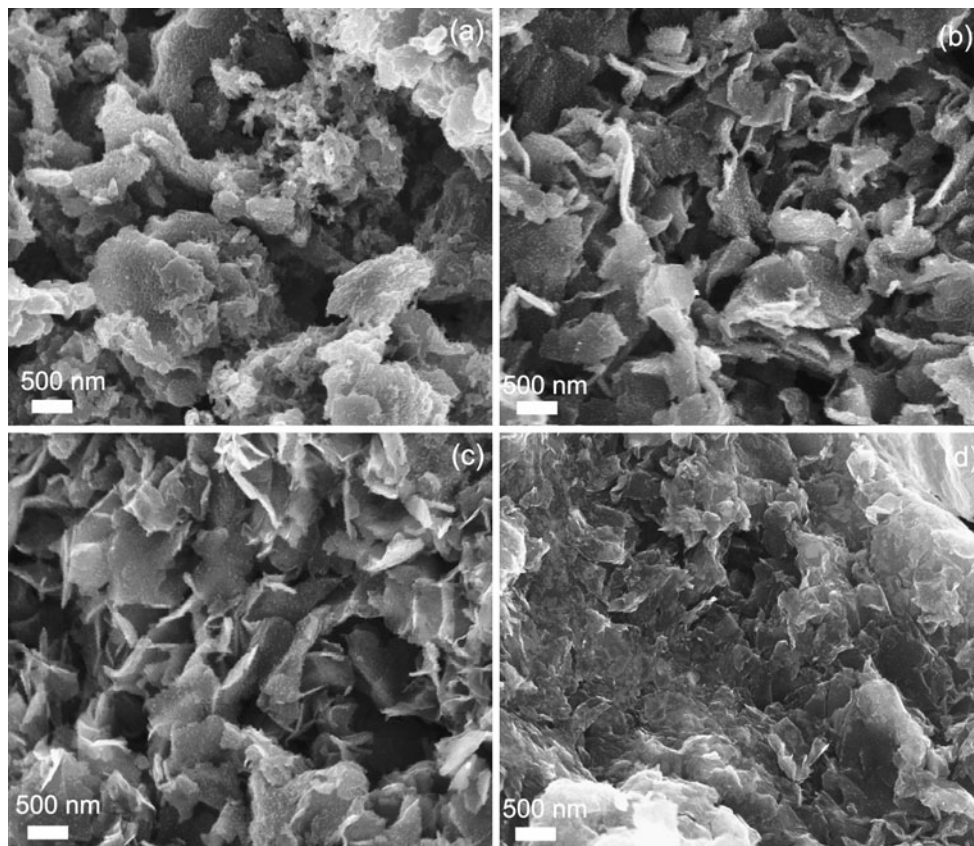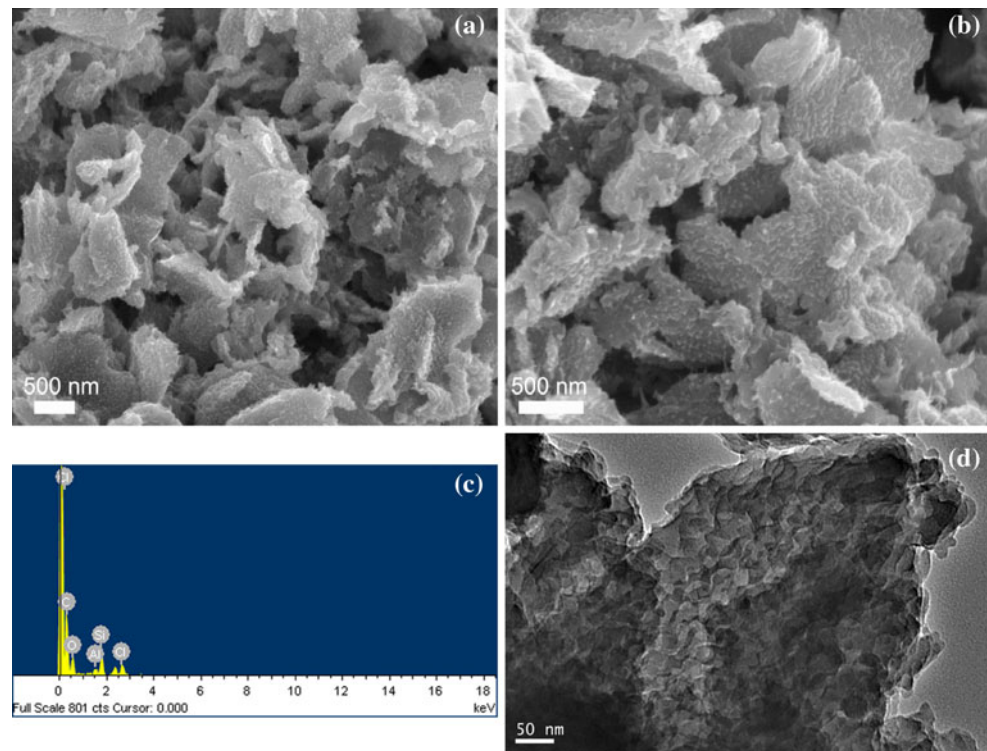

Fig. 5 SEM images of PANI/MMT with different MMT/aniline feeding ratio: **a** 12.5 %; **b** 50 %; **c** 75 %; **d** 100 %

Formation mechanism

Flake-like PANI/MMT composites were synthesized by in situ chemical oxidation polymerization, as illustrated in Fig. 7. First, Na^+-MMT was modified by GMA-DEA. After modification, hydroxyl groups and polymerizable double bond existed on the surface of the silicate platelets, which not only help GMA-DEA-MMT well disperse in water but also promote the grafting reaction of AMPS on the clay surface by solution polymerization. The synthesized poly(AMPS)-g-MMT dispersed in aqueous solution served as templates for adsorption of aniline monomer due to charge–charge interactions between the positively charged amine of the monomer and the negatively charged poly(AMPS) on the clay surface when aniline monomer was added. After introduction of APS oxidant, PANI/MMT composites with flake-like structure were prepared by in situ chemical oxidation polymerization during which poly(AMPS), a polymer acid, on the surface of clay platelets is used as dopant of PANI and play a 'bridge' role to combine PANI with clay.

Removal of Cr(VI) ions

It is well known that PANI or its composites can be used as effective adsorbents to remove Cr(VI) from water [21–28]. However, the effect of the morphology of PANI/MMT composites on the Cr(VI) adsorption has not been studied. Herein we used flake-like PANI/MMT composites as adsorbents for removal of Cr(VI) and demonstrated that PANI/MMT composites with flake-like morphology exhibited a high adsorption capacity. Results shown in Fig. 8 indicate that the PANI/MMT composites are able to remove Cr(VI) from aqueous solution. Furthermore, the

adsorption efficiency was closely related to feeding ratio of MMT to aniline. The MMT/aniline feeding ratio could affect the morphology of PANI/MMT composites. The variation of PANI/MMT morphology affected the removal efficiency of the composites by changing the interface between the composite and the solution. The maximum removal efficiency occurred when feeding ratio of MMT to aniline was 25 %. PANI/MMT composites with MMT/aniline feeding ratio of 25 % have uniform flake-like structure and rough surface, which can provide enough active sites to adsorb heavy metal ions, and were selected for further adsorption study.

Effect of pH on adsorption

Initial solution pH is one of the most important parameters in the heavy metal adsorption process. The effect of solution pH on Cr(VI) removal by the PANI/MMT composite
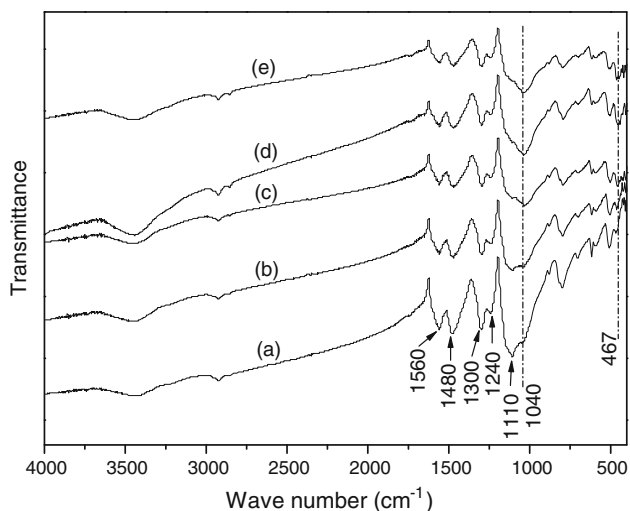

Fig. 7 Schematic illustration of the process of preparation flake-like PANI/MMT composites

Fig. 6 FTIR spectra of PANI/MMT with different MMT/aniline feeding ratio: (a) 12.5 %; (b) 25 %; (c) 50 %; (d) 75 %; (e) 100 %
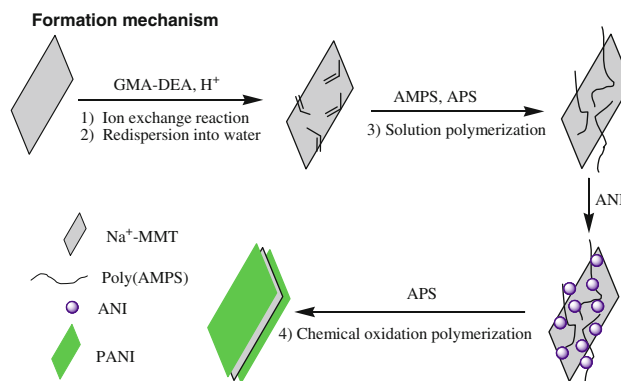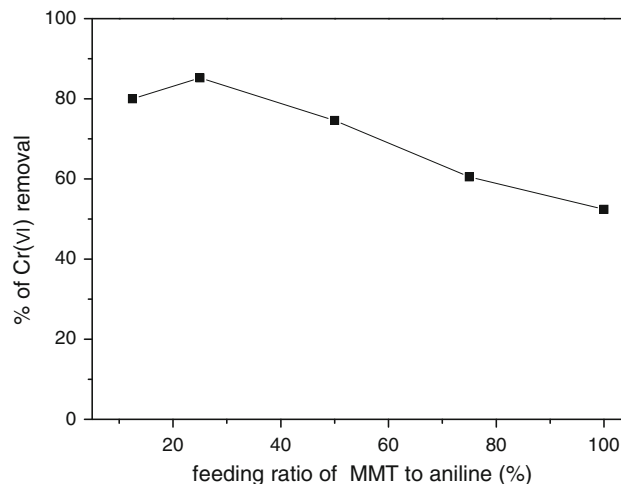

Fig. 8 Effect of feeding ratio of MMT to aniline on Cr(VI) removal using PANI/MMT composites (PANI/MMT dose 1 g/L; initial Cr(VI) 100 ppm; pH 4; agitation time 150 min)

is shown in Fig. 9. It is observed that Cr(VI) removal efficiency decreases gradually with increase in pH from 2 to 10 for the flake-like PANI/MMT adsorbent. The mechanism of Cr(VI) adsorption by the PANI/MMT at lower solution pH values seems to mostly occur via anion exchange process which happened between doped Cl^- ions in the adsorbent and the $HCrO_4^-$ or dichromate in the solution [1, 21].

Adsorption kinetics

Figure 10a indicates the results of adsorption kinetic experiments at different initial concentrations of Cr(VI), which were conducted to determine the optimum adsorption time. The rapid removal is due to the rough surface and easily accessible surface sites on the flake-like PANI/MMT. The equilibrium time also depends on the initial Cr(VI) concentrations. Specifically, the time to reach equilibrium increases from 5 to 120 min with an increase in initial concentration from 25 to 200 mg/L. In order to understand better the adsorption behaviors, the pseudo-second-order model which is dependent on the amount of solute adsorbed on the surface of adsorbent and the amount adsorbed at equilibrium was applied to test the adsorption experimental data:

$$\frac{t}{q_t} = \frac{1}{k_2 q_e^2} + \frac{t}{q_e}, \qquad (5)$$

where k_2 is the rate constant (g/mg min). The result (seen in Fig. 10b) shows that t/q_t versus t is linear for PANI/MMT at different initial Cr(VI) concentrations. q_e, k_2 and correlation coefficient R^2 were calculated and listed in Table 1. It is observed that the correlation coefficient R^2 for pseudo-second-order kinetic model is above 0.999 and the
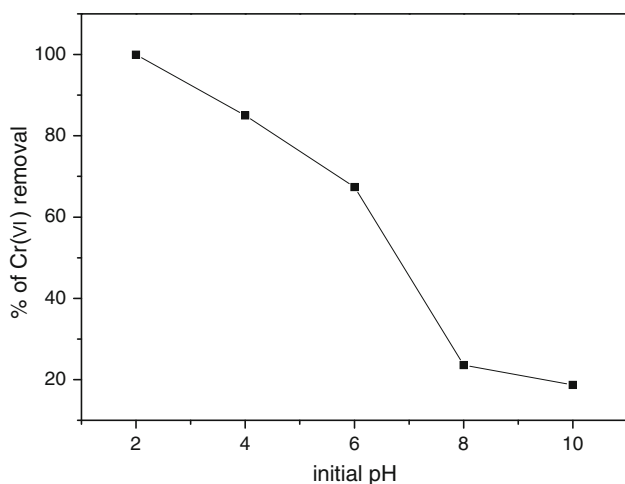
calculated values of $q_{e,cal}$ for pseudo-second-order kinetic model are in good agreement with the experimental values of $q_{e,exp}$, indicating that the adsorption process follows the pseudo-second-order kinetics.

Adsorption isotherms

The equilibrium adsorption isotherm is fundamental in describing the interactive behavior between solutes and adsorbent and is important for the design of adsorption system. The initial concentration of Cr(VI) adsorption has obvious effect on the Cr(VI) adsorption. The adsorption capacity increased with the increase of initial Cr(VI) concentration from 25 to 250 mg/L (shown in Fig. 11a), which may be due to the extent of a driving force of concentration gradients with the increase in the Cr(VI) concentration [27]. Three extensively used isotherm models viz. Langmuir, Freundlich, and Temkin models were employed to investigate the isotherm data. The linear isotherm equations are expressed as follows:
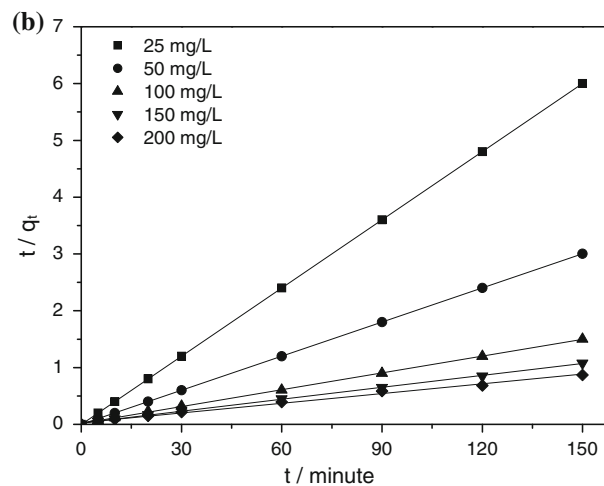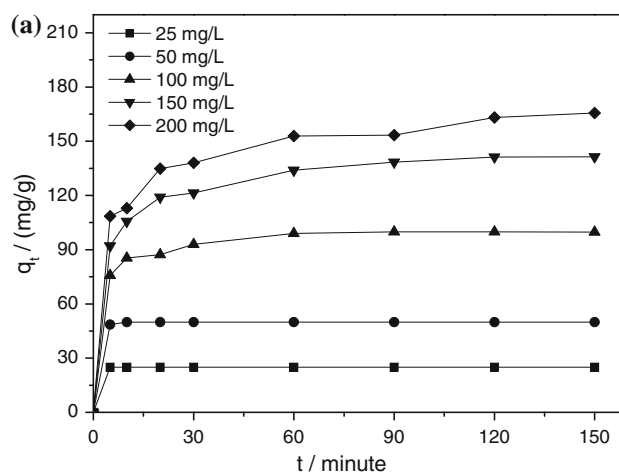

Fig. 9 Effect of pH on the adsorption of Cr(VI) by the flake-like PANI/MMT (PANI/MMT dose 1 g/L; initial Cr(VI) 100 ppm; agitation time 150 min)

Fig. 10 a Adsorption kinetics curves and b pseudo-second-order kinetic plots for the adsorption of Cr(VI) at different initial concentrations

Langmuir: $\dfrac{C_e}{q_e} = \dfrac{1}{q_m b} + \dfrac{C_e}{q_m}$ (6)

Freundlich: $\ln q_e = \ln k_F + \dfrac{1}{n} \ln C_e$ (7)

Temkin: $q_e = A + B \ln C_e$,   (8)

where q_m and b are the Langmuir constants related to the adsorption capacity (mg/g) and the rate of adsorption

Table 1 Kinetics parameters for Cr(VI) adsorption onto the flake-like PANI/MMT

C_0 (mg/L)	$q_{e,exp}$ (mg/g)	$q_{e,cal}$ (mg/g)	k_2 (g/mg min)	R^2
25	24.99	24.99	49.00	1
50	49.94	49.95	0.852	1
100	99.81	101.01	0.00594	0.999
150	141.37	143.88	0.00214	0.999
200	165.59	167.22	0.00147	0.999

(L/mg), respectively; k_F and n are the Freundlich isotherm parameters related to adsorption capacity (mg/g) and intensity of adsorption, respectively; and A and B are Temkin isotherm constants. The linearized Langmuir, Freundlich and Temkin isotherms are shown in Fig. 11b–d, respectively. The Langmuir, Freundlich, and Temkin isotherm parameters calculated from the slope and intercept of the linear equations are given in Table 2. The high values of correlation coefficient reveal that Langmuir model fitted well the isotherm data compared with other two models. A basic assumption of the Langmuir theory is that the sorption takes place at specific homogeneous sites on the adsorbent. By this, it implies that the adsorption of Cr(VI) on the surface of flake-like PANI/MMT nanocomposites occurred by monolayer formation, which further indicates the homogeneity of the PANI/MMT nanocomposites surface. The values of q_m is 167.5 mg/g, which is quite close to the experimental value shown in Table 1. This reveals that the
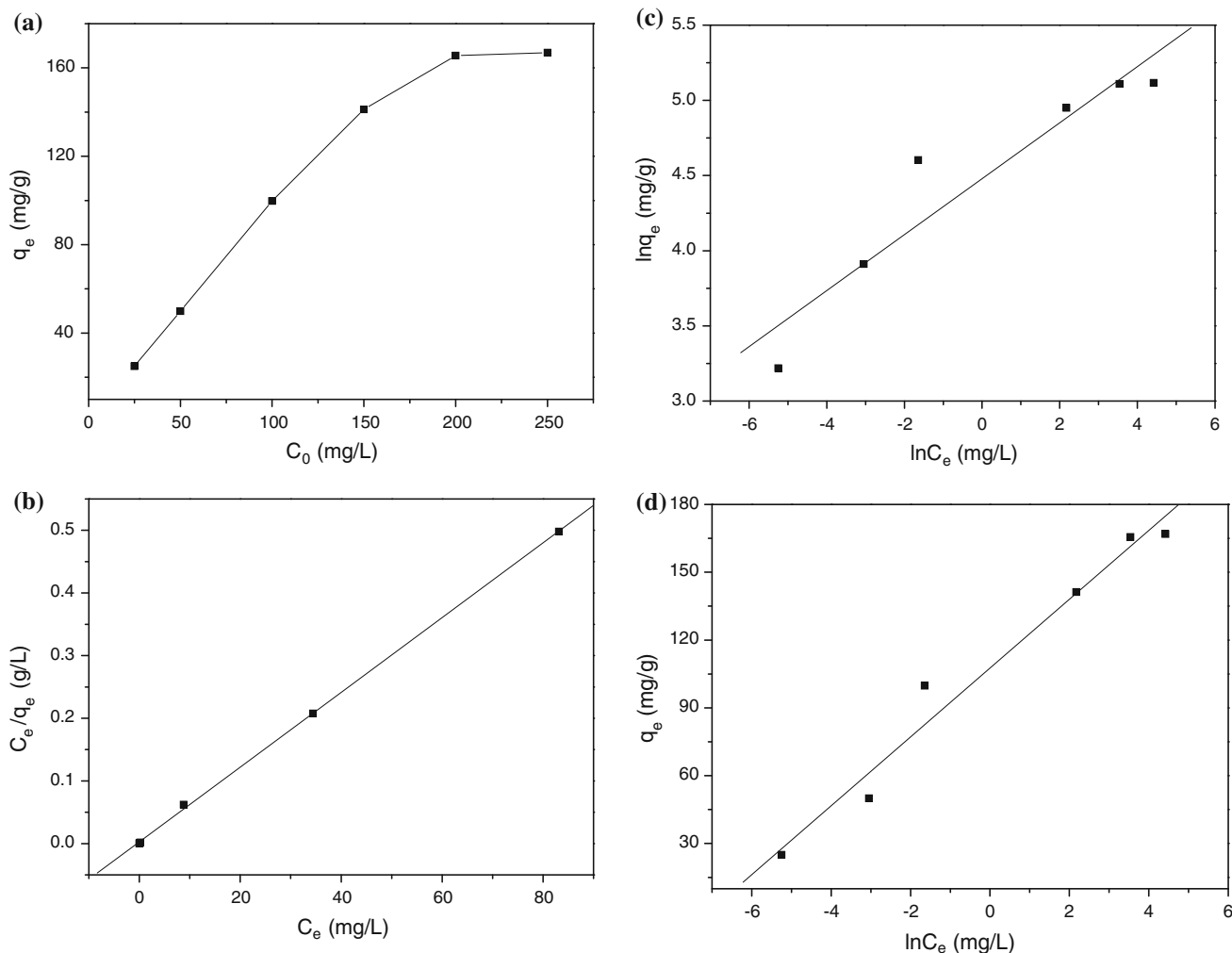

Fig. 11 **a** The plot of adsorption capacity against initial Cr(VI) concentration; **b** Langmuir adsorption isotherm, Freundlich adsorption isotherm **c** and Temkin isotherm **d** for Cr (VI) ions adsorption on the flake-like PANI/MMT

**Table 2** Parameters of the Langmuir, Freundlich, and Temkin isotherm models

Langmuir			Freundlich			Temkin		
q_{m} (mg/g)	b (L/mg)	R^2	k_{F} (mg/g)	n	R^2	A	B	R^2
167.5	2.27	0.999	88.16	5.52	0.947	107.59	15.23	0.986
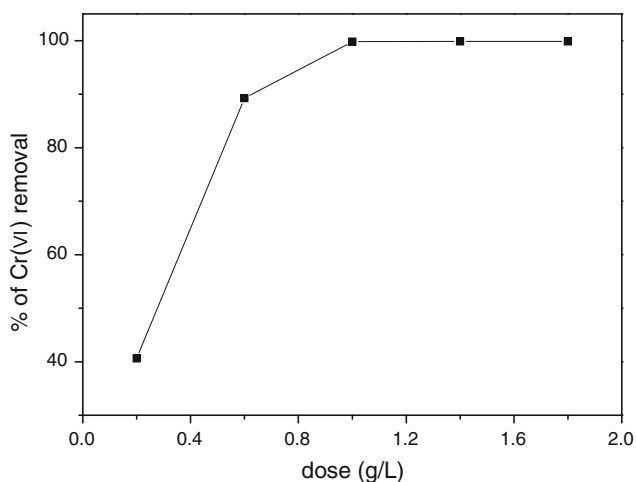
Fig. 12 Effect of adsorbent dose on the removal of Cr(VI) by the flake-like PANI/MMT (initial Cr(VI) 100 ppm; pH 2; agitation time 150 min)

as-synthesized PANI/MMT with flake-like morphology have a superior adsorption capacity, possibly due to its rough surface with larger specific surface area.

Effect of PANI/MMT dose

The effect of the flake-like PANI/MMT dose on the removal efficiency of Cr(VI) from solution was also studied (shown in Fig. 12). It is observed that the removal efficiency increased from 40.6 to 99.8 % with an increase in adsorbent dose from 0.2 to 1 g/L. This is due to the increase in the number of active sites available for adsorption. Afterward (from 1 g/L), the removal efficiency of Cr(VI) remains unchanged with increase in PANI/MMT dose because the Cr(VI) becomes limiting in the system. Compared with materials reported in literature, such as polyacrylonitrile/ferrous chloride composite nanofibers [35], polyaniline doped with sulfuric acid [21], and modified halloysite nanotubes [36], the flake-like PANI/MMT composites developed in this study exhibit better efficiency in the removal of Cr(VI) from aqueous solution.
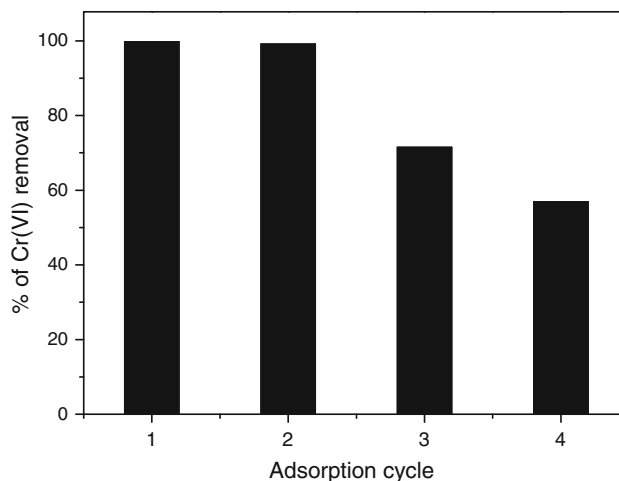
Fig. 13 Adsorption cycle

Desorption studies

Desorption efficiency of the PANI/MMT was evaluated by performing adsorption–desorption experiment for four consecutive cycles. Only 12.3 % of the adsorbed Cr(VI) was desorbed in the first cycle of desorption. A lower desorption efficiency was also observed for PPy-PANI nanofibers [1] and KF/PANI nanocomposites [27]. This is due to the reduction of adsorbed Cr(VI) to Cr(III) by PANI which could not be desorbed upon treatment with NaOH solution [1, 27]. The removal efficiency of PANI/MMT in each cycle of adsorption is shown in Fig. 13. It is observed that the removal efficiency (99 %) of PANI/MMT remained almost same for first two cycles and in the subsequent third (72 %) and forth cycles (57 %) there are gradual decrease in the removal efficiency. This result indicated that the flake-like PANI/MMT adsorbent can be reused for two adsorption–desorption cycles without any loss of its removal efficiency.

Conclusions

In conclusion, a facile in situ chemical oxidation polymerization method was developed for the controllable synthesis of flake-like PANI/MMT composites with rough surface in aqueous solution. In this synthesis system, clay platelets carrying poly(AMPS) on the surface, which can be used as dopant of PANI and play a 'bridge' role to combine PANI with clay, served as templates to guide the growth orientation of PAN by which PANI/MMT with flake-like shape were developed. When the as-synthesized PANI/MMT were used as absorbents for Cr(VI) removal from aqueous solution, the adsorption kinetics and isotherms were well described by pseudo-second-order and

Langmuir models, respectively. Importantly, flake-like PANI/MMT exhibited high efficiency to adsorb Cr(VI) from aqueous solution with the maximum adsorption capacity up to 167.5 mg/g. This work not only provides a facile approach for designing and developing PANI/MMT composites with unique micro/nanostructures but also gives a promising adsorbent for heavy metal ions.

References

1. Bhaumik M, Maity A, Srinivasuc VV, Onyango MS (2012) Chem Eng J 181–182:323
2. Esmaeili A, Meddaghinia A, Vazirinejad R (2005) Am J Appl Sci 2:1471
3. Rengaraj S, Joo CK, Kim Y, Yi J (2003) J Hazard Mater 105:257
4. Shi T, Wang Z, Liu Y, Jia S, Du C (2009) J Hazard Mater 2–3:900
5. Kozlowski CA, Walkowiak W (2002) Water Res 36:4870
6. Sun L, Zhang L, Liang C, Yuan Z, Zhang Y, Xu W, Zhang J, Chen Y (2011) J Mater Chem 21:5877
7. Chabaane L, Tahiri S, Albizane A, El Krati M, Cerver ML, de la Guardi M (2011) Chem Eng J 174:310
8. Fu F, Wang Q (2011) J Environ Manage 92:407
9. Anupam K, Dutta S, Bhattacharjee C, Datta S (2011) Chem Eng J 173:135
10. Duranoğlu D, Trochimczuk AW, Beker U (2012) Chem Eng J 187:193
11. Ali IO, Thabet MS, El-Nasser KS, Hassan AM, Salama TM (2012) Micropor Mesopor Mat 160:97
12. Bhattacharyya KG, Gupta SS (2006) Ind Eng Chem Res 45:7232
13. Bhattacharyya KG, Gupta SS (2008) Adv Colloid Interface 140:114
14. Misra RK, Jain SK, Khatri PK (2011) J Hazard Mater 185:1508
15. Wu Z, Li S, Wan J, Wang Y (2012) J Mol Liq 170:25
16. Wan Ngah WS, Teong LC, Hanafiah MAKM (2011) Carbohydr Polym 83:1446
17. Banarjee SS, Joshi MV, Jayaram RV (2004) Sep Sci Technol l39:1611
18. Lakatos J, Brown SD, Snape CE (2002) Fuel 81:691
19. Bhadra S, Khastgir D, Singha NK, Lee JH (2009) Prog Polym Sci 34:783
20. Deng SB, Ting YP (2005) Environ Sci Technol 39:8490
21. Zhang R, Ma H, Wang B (2010) Ind Eng Chem Res 49:9998
22. Chowdhury P, Roy K, Mondal P (2008) J Polym Mater 25:589
23. Guo X, Fei GT, Su H, Zhang LD (2011) J Phys Chem C 115:1608
24. Li Q, Sun L, Zhang Y, Qian Y, Zhai J (2011) Desalination 266:188
25. Chowdhury P, Mondal P, Roy K (2011) J Appl Polym Sci 119:823
26. Lashkenari MS, Davodi B, Ghorbani M, Eisazadeh H (2012) High Perform Polym 24:345
27. Zheng Y, Wang W, Huang D, Wang A (2012) Chem Eng J 191:154
28. Kumar PA, Chakraborty S (2009) J Hazard Mater 162:1086
29. Bhattacharyya KG, Gupta SS (2007) Ind Eng Chem Res 46:3734
30. Qu J, Cao CY, Hong YL, Chen CQ, Zhu PP, Song WG, Wu ZY (2012) J Mater Chem 22:3562
31. Li H, Li W, Zhang Y, Wang T, Wang B, Xu W, Jiang L, Song W, Shu C, Wang C (2011) J Mater Chem 21:7878
32. Abd El-Ghaffar MA, El-Halawany NR, Ahmed SA (2010) J Appl Polym Sci 115:3063
33. Unnithan MR, Anirudhan TS (2001) Ind Eng Chem Res 40:2693
34. Kang ET, Neoh KG, Tan KL (1998) Prog Polym Sci 23:277
35. Lin Y, Cai W, Tian X, Liu X, Wang G, Liang C (2011) J Mater Chem 21:991
36. Wang J, Zhang X, Zhang B, Zhao Y, Zhai R, Liu J, Chen R (2010) Desalination 259:22